Published by SET Publisher

Journal of Pharmacy and Nutrition Sciences

ISSN (online): 1927-5951

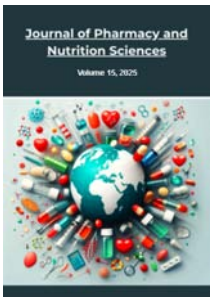

Onion Peel-Derived Exosome-Like Nanovesicles as a Novel Therapeutic Approach for Inflammatory Bowel Disease

Fabrizia Sepe[1,†,*], Anna Valentino[1,†], Youssra Lefrioui[2], Sabrina Margarucci[1], Orsolina Petillo[1], Loredana Marcolongo[1], Dalila Bousta[2,3], Anna Calarco[1,*] and Raffaele Conte[1]

[1]*Research Institute on Terrestrial Ecosystems (IRET)-CNR, Via Pietro Castellino 111, 80131 Naples, Italy*

[2]*Laboratory of Biotechnology Environment Agrofood and Health (LBEAS), Faculty of Sciences Dhar El Mahraz, Sidi Mohamed Ben Abdellah University, Fez 30000, Morocco*

[3]*National Agency of Medicinal and Aromatic Plants, 34025 Taounate, Morocco*

Article Info:

Keywords:
Allium cepa,
Plant-derived exosome-like nanoparticles,
Inflammatory Bowel Disease (IBD),
Intestinal epithelial barrier,
Waste valorization.

Timeline:
Received: July 07, 2026
Accepted: August 03, 2026
Published: August 21, 2026

Citation: Sepe F, Valentino A, Lefrioui Y, Margarucci S, Petillo O, Marcolongo L, Bousta D, Calarco A, Conte R. Onion peel-derived exosome-like nanovesicles as a novel therapeutic approach for inflammatory bowel disease. J Pharm Nutr Sci 2026; 16: 29-45.

DOI: https://doi.org/10.29169/1927-5951.2026.16.04

Abstract:

Chronic inflammation of the intestinal mucosa and impaired intestinal epithelial barrier integrity are two hallmarks of inflammatory bowel disease (IBD). Given the limitations and side effects of conventional biological therapies, the isolation of plant-derived exosome-like nanoparticles (PDEN) from agri-food byproducts represents a sustainable and biocompatible therapeutic option for the development of novel bioactive platforms. In this study, we successfully extracted nanovesicles from industrial onion (*Allium cepa*) waste peels (OP-EVs) using a protocol combining enzymatic digestion, differential centrifugation, and ultracentrifugation. Their stable nanoscale size (94.1 ± 1.7 nm mode; 63.0 nm), negative surface charge (-16.3 mV), plant-specific markers (Hsp70, TET8, PEN1), and high encapsulation of bioactive flavonoids and polyphenols were confirmed by NTA, DLS, Western blot and LC-MS/MS analysis. In human colonic epithelial cells (HCECs), OP-EVs were non-cytotoxic and efficiently internalized. OP-EVs significantly reduced pro-inflammatory cytokine production (IL-8, IL-6, and TNF-α) under LPS-induced acute inflammatory stress by reducing MAPK/ERK activation and NF-κB (p65). Additionally, OP-EVs restored E-cadherin expression, suppressed N-cadherin overexpression, and markedly accelerated scratch wound closure to protect mucosal barrier integrity in chronic inflammatory conditions. Collectively, these findings suggest that OP-EVs may represent a potential zero-waste nutraceutical platform capable of sustaining epithelial barrier integrity while lowering mucosal inflammation.

*Corresponding Author

E-mails: fabriziasepe@cnr.it; anna.calarco@cnr.it

†These authors contributed equally to this work.

INTRODUCTION

In recent decades, inflammatory bowel diseases (IBD), clinically expressed as ulcerative colitis (UC) and Crohn's disease (CD), have gained recognition as a worldwide health issue, with an increasing incidence throughout the world [1]. IBD is characterized by a chronic, recurrent, and unpredictable course of inflammatory disease in the gastrointestinal tract, which severely impairs patients' quality of life [2]. The precise etiology of these diseases is unknown; however, it is known that the pathogenesis of IBD is triggered by a complex and dysfunctional interaction of genetic predisposition, environmental stimuli, immune system dysregulation, and qualitative and quantitative changes in the intestinal microbiota (gut dysbiosis) [3].

Progressive impairment of intestinal epithelial barrier integrity is a key factor underlying the pathophysiology of IBD, which aggravates cellular infiltration, tissue damage, and a cascade of mucosal inflammatory responses [4]. In the healthy gut, selective permeability is modulated by a single layer of epithelial cells joined by tight junction proteins such zonula occludens (ZO-1), occludin, and claudins, which prevent luminal agents and pathogens from entering the lamina [5]. The highly sensitive intestinal barrier is structurally compromised in IBD, leading to a phenomenon known as "leaky gut". This results in a constant input of luminal antigens and persistent activation of local immunological and epithelial cells. Prolonged activation results in high levels of pro-inflammatory cytokines (e.g. TNF-α, IL-1β, and IL-6) and reactive oxygen species (ROS), contributing to tissue damage and persistent mucosal inflammation [6,7].

Currently, the primary treatment options available for the management of IBD include anti-inflammatory medications, immunosuppressants, and biological treatments, such as anti-TNF- α monoclonal antibodies [8]. Although these interventions can achieve clinical remission, they frequently fail to promote long-term mucosal repair or actively restore the damaged epithelial barrier. Furthermore, these therapies have important drawbacks, which include high main and secondary failure rates, high costs, and severe systemic adverse effects, such opportunistic infections and cancer [9,10]. Therefore, it is essential to identify novel, non-toxic, and biocompatible bioactive compounds capable of selectively targeting the inflamed intestinal mucosa while preserving epithelial barrier integrity and lowering the chronic inflammatory cascade.

Extracellular vesicles (EVs) are new cellular and inter-organismal communication agents that emerged in the intestinal milieu [11].

EVs are small, nanometer-sized objects encased in a lipid bilayer that can carry proteins, lipids, and short RNAs to recipient cells, thereby controlling mucosal homeostasis and immunological tolerance. While mammalian and microbial EVs have been extensively explored for their regulatory role in immune response and microbial regeneration, plant-derived exosome-like nanoparticles (PDENs) represent a novel frontier in nutraceuticals and targeted drug delivery systems [12,13].

PDENs, in fact, have several inherent advantages over synthetic nanocarriers, including biocompatibility, low toxicity, oral stability, and the capacity to safely penetrate the gastrointestinal tract to reach inflamed mucosal regions [14].

In addition, the valorization of agricultural byproducts and the consumption of functional foods are well aligned with the objectives of sustainable pharmaco-therapy and the circular economy. Onion peels (*Allium cepa L.*) are a common industrial waste product and contain bioactive secondary metabolites with strong antioxidant and anti-inflammatory activities, such as quercetin glycosides and organosulfur compounds [15]. The isolation and extraction of PDENs from onion peels may be a promising therapeutic strategy [16], for valorizing this waste material while exploiting the biological activity of onion-derived phytocompounds.

Onion peel-derived exosome-like nanovesicles (OP-EVs) represent a sustainable zero-waste approach that repurposes an abundant agro-industrial byproduct, whereas much of the research on PDEVs has focused on fresh, edible tissues, such as grape, ginger, or grapefruit. Importantly, the outer protective peels of *Allium cepa* have a distinctive phytochemical profile enriched in polyphenolic compounds. Compared to traditional PDEV platforms, this may provide a distinctive combination of phytochemical-associated stability and anti-inflammatory and barrier-protective activities. Although onion-derived nanoparticles have previously been reported [17], the specific use of onion peel as a source of exosome-like nanovesicles and their effects on human intestinal epithelial inflammation and barrier repair remain comparatively unexplored.

The purpose of this study was to explore the anti-inflammatory properties of PDENs derived from *Allium cepa* waste peels in an *in vitro* model of IBD.

Using human colon epithelial cells (HCECs) treated with lipopolysaccharide (LPS), we investigated the ability of these nanovesicles to mitigate inflammatory responses and promote epithelial repair. Finally, we investigated their potential molecular mechanism of action, focusing on the regulation of NF-κB and ERK signaling pathways, as well as their effects on epithelial wound closure and E-cadherin/N-cadherin expression.

2. MATERIALS AND METHODS

2.1. Materials

P. gingivalis ultrapure lipopolysaccharide (LPS) (1ug/mL, Cat. No. L2880-10MG, Sigma-Aldrich, Milan, Italy), Phosphate-buffered saline (PBS) (Cat. No. P4474-500ML), DAPI nuclear stain (Cat. No. 5087410001), paraformaldehyde (Cat. No. P6148-500G) and lipophilic fluorescent membrane linker kit PKH67 (Cat. No. MIDI67-1KT) were purchased from Sigma Aldrich (Milan, Italy).

For Western blot analysis, cOmplete™, EDTA-free Protease Inhibitor Cocktail (Cat. No. 11836170001), PhosSTOP™ (Cat. No. 4906837001), Bovine Serum Albumin (Cat. No. A7030), and Immobilon Crescendo Western HRP substrate (Cat. No. WBLUR0500) were purchased from Merk Life Science S.r.l. (Milan, Italy). DC™ Protein Assay Kit II (Cat. No. 5000111), 4× Laemmli Sample Buffer (Cat. No. 1610747), Nitrocellulose Membrane 0.2 µm (Cat. No. 1620112), and Non-Fat Dry Milk (Cat. No. 10004504) were purchased from Bio-Rad Laboratories (Milan, Italy). Pierce BCA protein assay kit (Cat. No. 23227) was procured from Thermo Scientific (Waltham, MA, USA). Radioimmunoprecipitation assay buffer (RIPA buffer, Cat. No. 9806), total NF-κB (Cat. No. 8242S), phosphorylated NF-κB (Cat. No. 3036S), total ERK (Cat. No. 9102S), phosphorylated ERK (Cat. No. 9201L), and E-cadherin (Cat. No. 14472S) were purchased from Cell Signalling Technology Inc. (Danvers, MA, USA). N-cadherin (Cat. No. E-AB-70061) was purchased from Elabscience Biotechnology Co. (Wuhan, Hubei, Cina). Primary antibodies directed against plant-specific markers Hsp70 (Cat. No. PHY0167), TET8 (Cat. No. PHY1491S), and PEN1(Cat. No. PHY2912A)) were purchased from PhytoAB Inc. (San Jose, CA, USA). Goat anti-rabbit IgG (Cat. No. sc-2004), and anti-mouse IgG (Cat. No. sc-2354), β-Actin (Cat. No. sc-47778) was acquired from Santa Cruz Biotechnology Inc. (Dallas, MA, USA). All other reagents were of analytical grade and, when not indicated, were purchased from Sigma-Aldrich. Certified onion (*Allium cepa* L.) samples were kindly provided by "Associazione Cipolla di Vatolla" (Vatolla, Salerno, Italy).

2.2. Isolation of Onion Peel-Derived Exosome-Like Nanoparticles (OP-EVs)

Onion (*Allium cepa L.*) peels (20g) were carefully dried in an oven at 37°C, cut into small pieces and then homogenized using a commercial blender. A volume five times the weight (100ml, 1:5, w/v) of extraction buffer (VIB: MES 20 mM, NaCl 100 mM, and $CaCl_2$ 2 mM, pH 7.4) was added. To facilitate cell wall degradation and maximize the release of apoplastic vesicles, the extraction was performed in concomitance with an enzymatic digestion by adding cellulase (3 g/100 mL; Cat. No. 4902279303, DuPont Industrial Biosciences, Wilmington, DE, USA) and pectinase (0.2 g/100 mL; Cat. No. 89216-50G, Sigma Aldrich, Milan, Italy), under continuous stirring overnight at room temperature. The mixture was processed according to a typical ultracentrifugation-based workflow for EV isolation (Scheme 1). Briefly, the suspension was centrifuged at 3000× g for 30 min to sediment the larger organelles, followed by centrifugation of the supernatant at 10000× g for 60 min to eliminate cell debris. The resulting supernatant was then centrifuged at 16000× g for 90 min to remove the aggregates and other cellular components. All centrifugation steps were performed at 4°C. The supernatant that emerged was passed through a 0.22 m syringe filter to eliminate any additional large particles. The filtrate was then ultracentrifuged (Optima LE-80K, Beckman Coulter, Brea, California) for 120 min at 4°C on a 70Ti rotor. Finally, the resultant pellet containing the OP-EVs was washed with sterile phosphate-buffered saline (PBS), ultracentrifuged again under same conditions and resuspended in PBS. To further concentrate the sample and eliminate low-molecular-weight contaminants, the vesicle suspension was subjected to a centrifugal ultrafiltration at 3000× *g* for 15 min (using a 100 kDa molecular weight cut-off membrane filter). To assess the effect of the ultrafiltration step on OP-EV preparation, aliquots were collected before and after ultrafiltration and analyzed by nanoparticle tracking analysis (NTA). For this comparison, 1 mL of the preparation was examined at each step. Particle concentration and size distribution were measured in the preparation obtained after enzymatic treatment and immediately before ultrafiltration and in the final preparation after ultrafiltration. The post-ultrafiltration

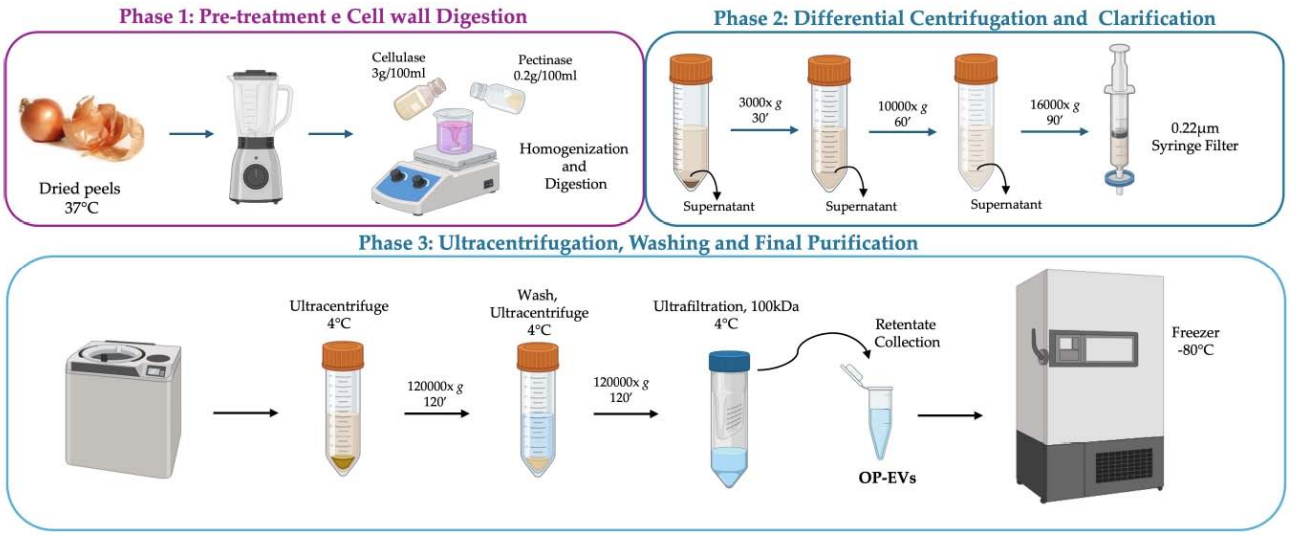

Scheme 1: Schematic representation of the extraction and purification workflow for onion peel-derived extracellular vesicles (OP-EVs).

preparation was employed in all subsequent physicochemical and biological experiments. The OP-EVs were then aliquoted and stored at -80°C for future analysis.

2.3. Physicochemical Characterization

The surface charge (zeta potential) of the isolated OP-EVs was assessed by Dynamic Light Scattering (DLS) using a Zetasizer (Ultra, Malvern Panalytical, Amesbury, UK). 10 µL of purified OP-EVs were diluted in 990 µL of filtered PBS and vortexed. To avoid aggregation, the entire volume was quickly placed into a disposable cuvette for size measurements. Three independent measurements were performed for each sample, and the analysis was processed by the software.

Particle size distribution profile and particle concentration (particles/mL) were captured using Nanoparticle Tracking Analysis (NTA) (Malvern Panalytical Ltd., Malvern, Worcestershire, UK) on a NanoSight platform. Prior to analysis, samples were diluted in particle-free, sterile-filtered PBS to achieve an optimal particle concentration range. Five videos of typical 60 s duration were recorded for each sample. Data were analyzed using NanoSight NTA software version 3.2, which was optimized to first identify and then track each particle on a frame-by-frame basis with a 488 nm laser. The temperature was maintained at 25 °C. Filtered PBS (blank) was run as a negative control.

NTA also served as an additional quality control measure for the OP-EV preparation, monitoring particle concentration and size distribution before and after the ultrafiltration stage. Appendix Figure **A1** shows compared NTA profiles. All following physicochemical and biological analyzes were performed using the final post-ultrafiltration preparation.

2.4. Liquid Chromatography-Mass Spectrometry (LC-MS/MS) Compositional Analysis

To identify and quantify the bioactive phytochemicals encapsulated within OP-EVs, liquid chromatography coupled with tandem mass spectrometry (LC-MS/MS) was performed. Briefly, 80 mg of lyophilized OP-EVs were reconstituted in 1 mL of HPLC-grade acetonitrile and sonicated in an ultrasonic bath for 60 min at 45 °C to ensure complete vesicle lysis and metabolite extraction. Prior to injection, the extracted sample was diluted with acetonitrile (1:2 v/v) and filtered through a 0.22 µm PTFE syringe filter.

Chromatographic separation and mass spectrometric detection were carried out using a Shimadzu ultra-high-performance liquid chromatograph (Nexera XR) coupled to a triple quadrupole LC-MS/MS detector (LCMS-8060, Shimadzu Italy, Milan, Italy). Chromatographic separation was achieved on a Kinetex C18 column maintained at 40 °C, using a gradient elution consisting of 0.1% (v/v) formic acid in water (Mobile Phase A) and 0.1% (v/v) formic acid in acetonitrile (Mobile Phase B) at a flow rate of 0.3 mL/min. Electrospray ionization (ESI) was operated in both positive and negative ion modes using multiple reaction monitoring (MRM) mode for accurate structural identification and relative quantification of targeted

flavonoids and phenolic compounds. Data acquisition and processing were performed using LabSolutions software (Shimadzu, Kyoto, Japan).

2.5. Validation of Plant-Specific Exosomal Markers via Western Blot

Proteins (50 µg) extracted from OP-EVs were loaded onto SDS-PAGE gels and electro-transferred onto PVDF membranes to validate their vesicular nature. The membranes were blocked with 5% bovine serum albumin (BSA) in TBST for 1 hour then probed overnight at 4°C with validated plant-specific primary antibodies, followed by incubation with HRP-conjugated secondary antibodies. Protein bands were captured using Immobilon Crescendo Western HRP Substrate and a ChemiDoc Imaging System (Bio-Rad Laboratories, Hercules, CA, USA). Antibodies used were Hsp70 (1:1000), TET8 (1:1000), and PEN1 (1:1000). Data collection and quantitative analysis were carried out with ImageJ software.

2.6. Cell Culture and Treatment

Human Colon Epithelial Cells (HCECs) were purchased from American Type Culture Collection (ATCC, Manassas, VA, USA) and were grown in Dulbecco's Modified Eagle Medium High Glucose (DMEM) supplemented with 10% fetal bovine serum (FBS), 2 mM L-glutamine, 100 U/ml penicillin-G and 100 mg/ml streptomycin (Euroclone, Milan, Italy). Cells were maintained in a humidified incubator at 37°C with 5% of CO_2. To establish *in vitro* pathological condition for IBD, confluent HCECs were stimulated with LPS for 30 and 60 min to detect early phosphorylation-dependent activation of NF-κB and MAPK/ERK signaling. The 60-minute time point was chosen for the comparison study because to the significant activation of NF-κB detected in the preliminary time-course evaluation, although phosphorylation signals were less visible at subsequent time points. Alternatively, cells were treated with a cocktail of INTF-γ (25ng/ml, Cat. No. SRP3058) and Il-1β (10 ng/ml, Cat. No. IL038) for 24h, to model chronic inflammatory conditions. Untreated cells maintained in complete medium served as negative controls, whereas cells exposed only to the inflammatory stimuli served as positive inflammatory controls.

2.6.1. Assessment of Cell Viability and Cytotoxicity

The effect of OP-EVs on HCEC viability was assessed using Cell Counting Kit-8 (Cat. No. 96992-100TESTS-F, Millipore Sigma, Milan, Italy). Briefly, HCEC cells were seeded in a 96-well plate at a density of 8 $\times 10^3$ (cells/well) and incubated overnight. Cells were subsequently subjected to a gradient of OP-EVs concentrations (from 10^7 to 10^9 particles/mL) for 24, 48 and 72 hours. This concentration range was selected to assess cytocompatibility over a broad range of vesicle exposure and to identify a suitable concentration for subsequent functional experiments. CCK-8 reagent (10 µL/well) was then added and the plates were incubated for an additional 2 hours at 37°C, following the manufacturer's procedure. The absorbance was measured at 450 nm with a Citation 5 Cell Imaging Multi-Mode microplate reader (BioTek, Bad Friedrichshall, Germany). Cell viability was expressed as a percentage relative to the untreated control cells.

To evaluate cell membrane integrity and cytotoxicity, lactate dehydrogenase (LDH) release into the culture medium was measured. Briefly, after the indicated treatment times, cell-free culture supernatants were collected and processed using a commercial LDH assay kit (Cat. No. MAK464, Sigma-Aldrich, Milan, Italy) according to the manufacturer's protocol. Total LDH release (100% cytotoxicity) was determined by lysing cells with 1% Triton X-100 (Cat. No. X100-5ML, Sigma-Aldrich, Milan, Italy). Absorbance was measured at 490 nm using the Cytation 5 microplate reader. The percentage of cytotoxicity was calculated relative to the total LDH release control.

Based on the CCK-8 and LDH results, 10^8 particles/mL was selected for the subsequent experiments, as cell viability remained comparable to that observed at 10^9 particles/mL, indicating a plateau in the response, while requiring a lower amount of OP-EV preparation.

2.6.2. Cellular Internalization and Wound healing

To track the vesicles' entrance and intracellular localization, OP-EVs were fluorescently marked with the lipophilic green dye PKH67 according to the manufacturer's instructions. To prepare the final 2x dye solution, 4 µL of the ethanolic PKH67 dye solution was added to 1 mL of diluent C and incubated with OP-EVs for 10 minutes. To remove unbound dye, labeled vesicles were washed in sterile PBS and then ultracentrifuged at 120,000× g for 60 minutes at 4° C. Labeled PDENs (10^8 particles/mL) were incubated with HCECs for 24 hours at 37°C. Cells were further fixed with 4% paraformaldehyde, the membranes permeabilized, and the nuclei stained with DAPI. A Zeiss Axio fluorescence microscope (Colibrì LED light source) with FITC (green) and DAPI (blue) filters was

used to visualize and image cellular uptake kinetics. The images were taken at 40x magnification. A 24 h incubation period was selected to allow sufficient time for cellular internalization of OP-EVs and to evaluate their intracellular uptake under the experimental conditions used. The wound healing activity of HCECs was assessed utilizing an *in vitro* scratch assay. Briefly, HCECs were seeded in 6-well plates and grown until they formed a confluent monolayer. A sterile pipette tip was then used to make a linear scratch over the cell monolayer. The wells were gently cleaned with PBS to remove unattached cells before being imaged immediately following scratching (0 h). To determine the impact of acute inflammation and OP-EVs on epithelial wound closure, three experimental conditions were analyzed: untreated control cells, cells stimulated with LPS (1 μ g/mL) for 60 min, and cells stimulated with LPS (1 μ g/mL) for 60 min followed by treatment with OP-EVs at 10^8 particles/mL. Images of cell migration were acquired using an inverted microscope (ZOE Fluorescent Cell Imager, Bio-Rad Laboratories, Hercules, CA, USA) at 0 and 24 hours, and the cell migration rate was analyzed using ImageJ software (version 1.8.0, United States). To calculate the average value of the area between cells, lines were randomly drawn in the wound area. The migration rate is calculated as [(Area control 0h - Area treatment 12h or 24h) / Area control 0h] × 100%. Three independent experiments were performed for each experimental condition.

2.6.3. Quantification of Inflammatory Cytokines by ELISA

Concentrations of Interleukin-8 (IL-8; Cat. No. EZHIL8), Interleukin-6 (IL-6; Cat. No. EZIL6), and Tumor Necrosis Factor- α (TNF-α; Cat. No. EZHTNFA) in HCEC culture supernatants were quantified using commercial ELISA kits (Sigma-Aldrich, Milan, Italy), according to the manufacturer's instructions. Absorbance was measured using a microplate reader, and cytokine concentrations were calculated by interpolation from the respective standard curves.

2.6.4. Inflammatory Pathway Characterization via Western Blotting

Following the outlined treatment methods, HCECs were collected, washed with ice-cold PBS, and lysed in ice-cold RIPA buffer containing protease and phosphatase inhibitor cocktails. Cell lysates were sonicated and centrifuged at 14,000× g for 15 min at 4 °C, and the supernatants were kept at −80 °C until use. The DC protein assay kit was used to determine protein concentration. The samples were prepared with 4× Laemmli sample buffer and heated for 5 min. Equal protein amounts (50 μg) were separated via SDS-PAGE and transferred onto PVDF membranes. Membranes were blocked and immunoblotted overnight at 4°C with primary antibodies, then incubated by with a corresponding secondary antibody. Protein bands were observed with Immobilon Crescendo Western HRP Substrate and a ChemiDoc Imaging System (Bio-Rad Laboratories, Milan, Italy). A selection of antibodies was used: rabbit NF-κB (1:1000), mouse phosphorylated NF-κB (1:1000), rabbit ERK (1:1000), rabbit phosphorylated ERK (1:1000), mouse E-cadherin (1:1000) and rabbit N-cadherin (1:1000). Expression levels were recorded, normalized against β -actin (1:20k) from the same blot. ImageJ software was employed to do densitometric quantification.

2.7. Statistical Analysis

All experiments were performed using at least three independent biological replicates (n = 3), where each biological replicate originated from an independent isolation batch of OP-EVs. For the CCK-8, LDH, and ELISA assays, each independent experiment included eight technical replicate wells per experimental condition (n = 8 wells/condition). Cellular uptake, scratch wound healing, and Western blot experiments were independently repeated three times. Quantitative data are presented as mean ± Standard Error of the Mean (SEM), as specified in individual figure legends. All statistical calculations were carried out using the GraphPad Prism 10.0 software (GraphPad Software, San Diego, CA, USA). One-way ANOVA was performed to analyze statistical differences, followed by Tukey's post-hoc test for multiple comparisons. Significance levels are shown as * $p < 0.05$, ** $p < 0.01$, *** $p < 0.001$ and ****$p< 0.0001$.

3. RESULTS AND DISCUSSION

3.1. Isolation, Physicochemical Characterization, and Phytochemical Analysis of Onion Peel-Extracellular Vesicles (OP-EVs)

In recent years, the isolation of plant-derived exosome-like nanoparticles (PDENs) has gained considerable importance in the fields of sustainable pharmacology and green economy [13]. To obtain high-purity nanovesicles free of cellular debris and pectin-rich structures, standard isolation techniques require for differential ultracentrifugation coupled with enzymatic

digestion and downstream ultrafiltration [16]. Extracellular vesicles produced from onion (Allium cepa) have been shown to be structurally stable and capable of encapsulating native secondary metabolites [17]. Based on these experimental findings, onion-peel extracellular vesicles (OP-EVs) were successfully isolated from industrially processed onion peel waste.

Nanoparticle tracking analysis (NTA) confirmed the successful isolation of a nanosized particle population. The final suspension exhibited a size distribution, with a mean hydrodynamic diameter of 94.1 ± 1.7 and a modal diameter of 63.0 (Figure **1A**), values consistent with the dimensional range generally reported for plant-derived extracellular vesicles. These values are also consistent with size profiles thoroughly documented for other Allium species like garlic and leek [18,19]. To further examine the effect of the ultrafiltration step, NTA measurements were also performed before ultrafiltration, following enzymatic treatment. The pre-ultrafiltration preparation showed a mean particle diameter of 121.9 nm, a modal diameter of 117.1 nm, and a particle concentration of 7.63×10^{8} particles/mL. The final post-ultrafiltration concentration of the stable suspension was measured at $8.37 \times 10^{8} \pm 7.29 \times 10^{7}$ particles/mL. The comparative NTA profiles are reported in Appendix Figure **A1**. This distribution suggests that the combination of enzymatic digestion and ultrafiltration efficiently isolates intact nano-vesicles while discarding large macro-cellular contaminants. These data provide an additional assessment of the role of the ultrafiltration step on particle population and contribute in quality control of the final OP-EV preparation.

Furthermore, zeta potential investigation corroborated the structural stability and electrochemical surface characteristics typical of intact plant lipid bilayers. The OP-EV displayed a distinctly negative net surface charge with a mean zeta potential of -16.3 ± 0.5 mV (Figure **1B**), indicating a stable colloidal solution with a low aggregation propensity. Similar surface charges have been regularly documented for plant- derived EVs, reflecting the presence of negatively charged phospolipids and membrane-associated biomolecules [20].

In support of the structural characterisation, the phytochemical profile acquired via LC-MS/MS provides a direct structural explanation for the biological potency of OP-EVs. OP-EVs encapsulate a remarkably diverse phytochemical cargo, predominantly composed of flavonoids and phenolic acids (Figure **1C**, Table **1**). Among the detected metabolites, genistein (17.87%), baicalein (15.01%), naringenin derivatives (10.87%), formononetin (10.87%), hesperidin (8.15%), and luteolin derivatives (6.66%) represented the major constituents, whereas chlorogenic acid, ferulic acid, protocatechuic acid, catechin, and quercetin derivatives were detected at lower relative abundance. This profile shows that OP-EVs contain multiple bioactive compounds rather than a single predominant active substance. The encapsulation of these phytochemicals within the vesicular lipid bilayer may contribute to protecting them from degradation and oxidation, potentially improving their stability and cellular delivery compared with their free forms [21,22].

The identified phytochemical profile provides a molecular basis for the biological activity observed for onion-derived vesicles. From a mechanistic perspective, genistein and baicalein have been demonstrated to modulate MAPK/ERK phosphorylation, mitigating cellular stress and preventing cytokine-induced disassembly of mucosal tight junctions [23,24]. Naringenin and luteolin derivatives act as potent inhibitors of NF-κB nuclear translocation, directly suppressing the transcriptional upregulation of pro-inflammatory cytokines such as IL-6, IL-8, and TNF-α [25, 26]. Furthermore, phenolic acids like ferulic acid contribute to mucosal barrier repair by promoting E-cadherin expression and counteracting oxidative damage [27].

Although the contribution of individual metabolites cannot be established from the present study, the therapeutic efficacy of OP-EVs is best interpreted as the result of a potentially multi-target combined biological action. Rather than depending on a single active compound, OP-EVs' lipid bilayer serves as a natural nanocarrier, co-delivering a diverse variety of bioactive compounds while enhancing their stability and collective biological impact on human intestinal epithelial cells.

Western blot analysis further confirmed the vesicular identity and plant origin of the isolated OP-EVs (Figure **1D**). Plant vesicular markers, such as tetraspanin 8 (TET8), penetration protein 1 (PEN1), and heat shock protein (Hsp70), were all present in our samples. In plant biology, TET8 and the syntaxin PEN1 are recognized as canonical membrane markers involved in trafficking and exosome secretion at the plasma membrane-cell wall interface, particularly during defense responses [28], while Hsp70 plays a key role in vesicular protein sorting [29]. The detection of these

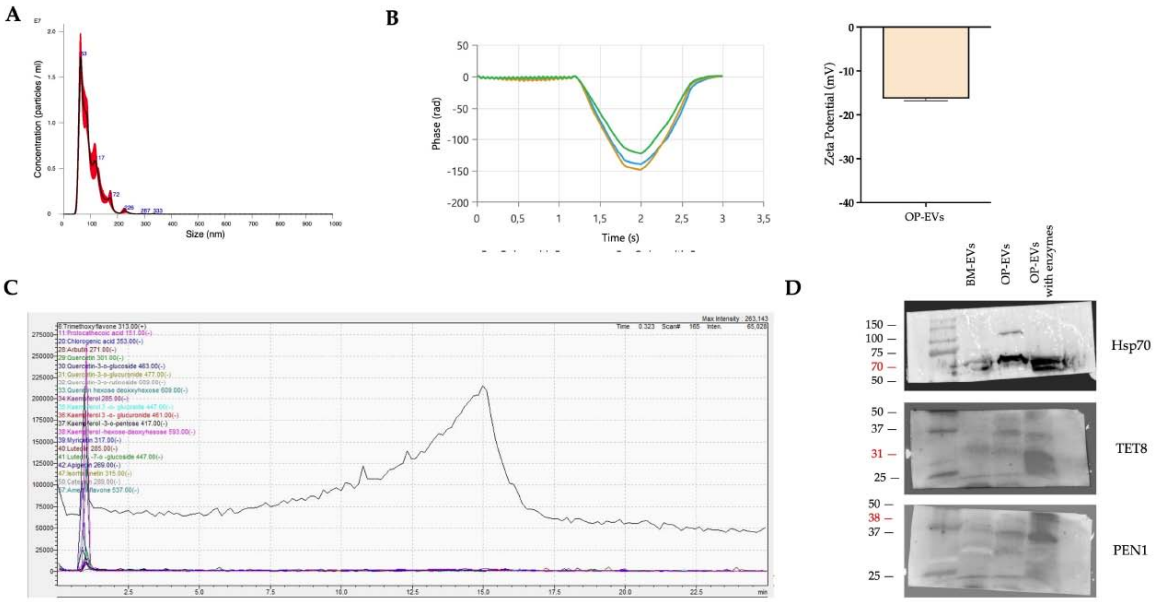

Figure 1: Physicochemical and molecular characterization of OP-EVs. (A) Nanoparticle Tracking Analysis (NTA) size and concentration distribution profiles of OP-EVs post-enzymatic digestion and ultrafiltration; **(B)** Zeta potential distribution and phase plot curves of OP-EVs in aqueous suspension; **(C)** Phytochemical profiling and mass spectrometry analysis of encapsulated secondary metabolites via LC-MS/MS. **(D)** Western blot analysis of Hsp70, TET8, and PEN1; bovine milk-derived extracellular vesicles (BM-EVs) were employed as a negative comparative control to assess antibody specificity and plant-ortholog enrichment.

Table 1: Qualitative and Semi-Quantitative LC-MS/MS Profiling of Bioactive Polyphenols Encapsulated in OP-EVs

Compound Name	Peak Area (AUC)	Relative Abundance (RA%)*
Hesperidin	1.20 x 10^6	8.15%
Naringenin derivatives	1.6 x 10^6	10.87%
Ferulic acid	8.50 x 10^5	5.78%
Chlorogenic acid	3.20 x 10^5	2.17%
Protocatechuic acid	1.80 x x10^5	1.22%
Quercetin aglycone	4.50 x 10^5	3.06%
Quercetin glycosides	1.13 x 10^5	0.77%
Kaempferol derivatives	5.10 x 10^5	3.47%
Isorhamnetin	2.40 x 10^5	1.63%
Genistein	2.63 x 10^6	17.87%
Baicalein	2.21 x 10^6	15.01%
Formononetin	1.60 x 10^6	10.87%
Luteolin & Luteolin-7-O-glucoside	9.80 x 10^5	6.66%
Apigenin	6.20 x 10^5	4.21%
Amentoflavone	4.10 x 10^5	2.79%
Trimethoxyflavone	3.50 x 10^5	2.38%
Catechin	2.10 x 10^5	1.43%

Relative Abundance (RA%) was calculated as the percentage of individual peak area (AUC) relative to the total integrated peak area (∑AUC) of all identified bioactive metabolites.

proteins therefore confirms the endosomal origin and vesicular identity of the isolated OP-EVs. Crucially, these specific plant orthologs were notably absent or highly depleted in the bovine milk-derived EV control (BM-EVs), underscoring the strict plant-specific signature of our isolated platform and minimizing the risk of cross-contamination artifacts [30].

Overall, the successful isolation of OP-EVs, together with their their nanoscale size, negative surface charge, enrichment in bioactive phytochemicals and canonical vesicular markers, provides a molecular framework for future evaluation of their biological effects in IBD models.

3.2. Biocompatibility and Internalization by Human Colon Epithelial Cells (HCECs)

The biocompatibility of PDEVs has been extensively reported, with low cytotoxicity observed in numerous mammalian cell models, including intestinal epithelial cells, suggesting their potential as safe natural nanocarriers for biomedical application [31]. Some examples include vesicles extracted from pomegranate (*Punica granatum*) which showed no change in the viability of colonic Caco-2 cells [32]; or EVs from cabbage and red cabbage exhibited no cytotoxicity when cultured with human skin cells and immune cell lines [33].

Therefore, the *in vitro* cytocompatibility of OP-EVs has been comprehensively evaluated on human colonic epithelial cells (HCECs), the primary cellular barrier impaired by inflammatory bowel disease (IBD). Cell viability was assessed by CCK-8 assay following exposure to a concentration gradient of OP-EVs (10^7, 10^8, and 10^9 particles/mL) for 24, 48 and 72 hours.

As shown in Figure **2A**, exposure to OP-EVs was not associated with any toxic effects across all tested concentrations and time points, remaining close to that of untreated controls (~100%). Intestinal epithelial cells survived even the greatest vesicle concentration (10^9 particles/mL) without substantial dose- or time-dependent reductions in viability. These findings reveal the cytocompatibility of OP-EVs and support their applicability for future therapeutic studies.

Measurement of LDH release was used to assess membrane integrity. Figure **2B** shows that OP-EVs did not cause detectable membrane damage at any tested concentration, but Triton X-100, used as a positive control, led to the expected maximum membrane rupture. These findings, combined with the CCK-8 data, show that OP-EVs are highly biocompatible and have no harmful effects on HCECs under the experimental settings used.

Aside from biocompatibility, the therapeutic efficacy of extracellular vesicles is dependent on their capacity to be properly internalized by recipient cells.

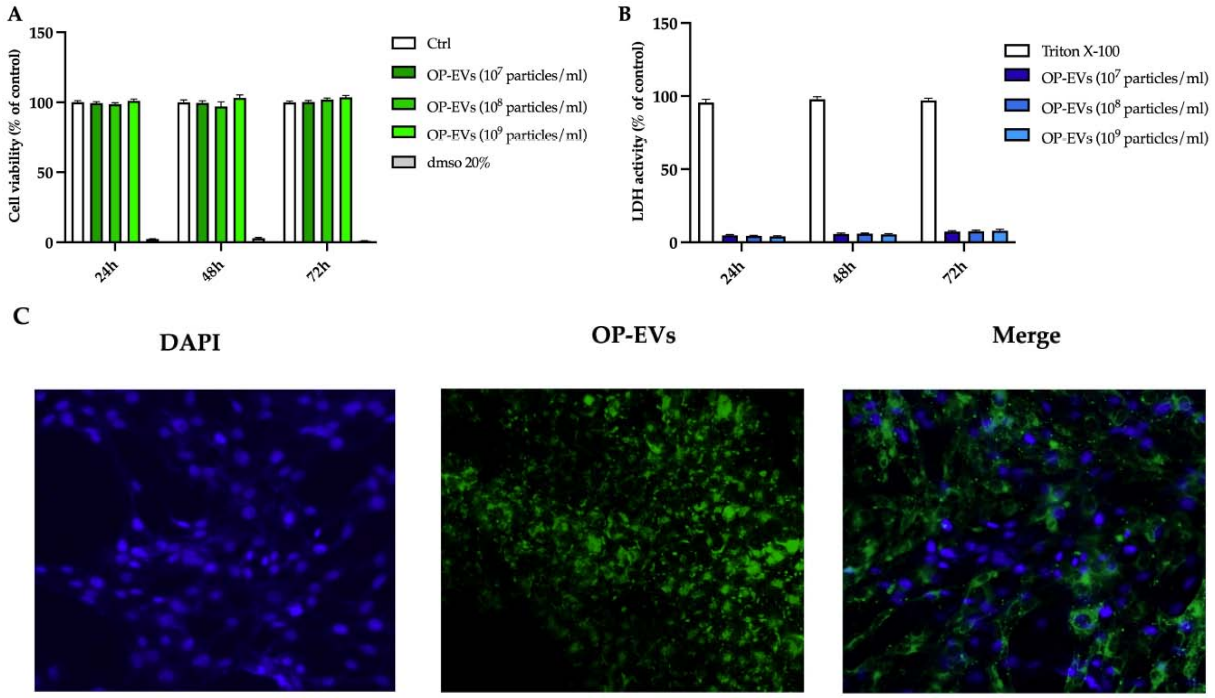

Figure 2: Biocompatibility and cellular uptake of OP-EVs in Human Colon Epithelial Cells (HCECs). (A) Cell viability measured by CCK-8 assay in HCECs exposed to increasing concentrations of OP-EVs (10^7, 10^8 and 10^9 particles/mL) for 24, 48, and 72 hours, using 20% DMSO as a positive control for cell death. **(B)** Membrane integrity evaluated by LDH release assay following OP-EV treatment. Triton X-100 was used as a positive cytotoxicity control. **(C)** Representative fluorescence microscopy images showing cellular uptake of green-labeled OP-EVs. Nuclei are counterstained with DAPI (blue, left). Data are expressed as mean ± SEM from n = 3 independent biological replicates.

To investigate the cellular uptake of OP-EVs, vesicles were fluorescently labeled with the lipophilic membrane dye PKH67 according to a previously optimized protocol for *Opuntia Ficus-indica*-derived extracellular vesicles (OFI-EV) [34] and incubated with HCECs for 24 h.

Fluorescence microscopy revealed that pure PKH67-OP-EVs were rapidly and efficiently internalized by HCECs (Figure **2C**). A unique green fluorescence dot pattern was mainly distributed throughout the cytoplasm, with a strong perinuclear localization, although no fluorescence was detected within DAPI-stained nuclei.

Efficient cellular internalization is required for the intracellular transport of vesicular bioactive cargo. The uptake observed in HCECs suggests that OP-EVs can effectively interact with intestinal epithelial cells and may function as naturally delivered nanocarriers for the delivery of bioactive compounds. These findings are consistent with previous studies revealing the effective uptake of plant-derived extracellular vesicles by human intestinal cells and their potential to mediate interkingdom communication through the intracellular transport of bioactive compounds [31].

3.3. OP-EVs Mitigate LPS-Induced Pro-inflammatory Cytokine Secretion in HCECs

Overproduction of pro-inflammatory cytokines and chemokines, including interleukin-8 (IL-8), interleukin-6 (IL-6), and tumor necrosis factor-alpha (TNF-α) is a major cause of chronic inflammation in intestinal mucosal diseases. These signaling molecules activate immune cell recruitment, promote mucosal injury, and disrupt epithelial tight junctions [35]. The immunomodulatory ability of OP-EVs was evaluated using an enzyme-linked immunosorbent assay (ELISA) on HCEC cells challenged with LPS.

Figure **3** shows that exposure to LPS significantly increased the secretion of all three pro-inflammatory mediators compared with untreated control cells (CTL). Specifically, IL-8 secretion grew from a baseline value of ~40 pg/mL up to ~830 pg/mL (Figure **3A**). Similarly, IL-6 production escalated from ~15 pg/mL to ~265 pg/mL (Figure **3B**), while TNF-α release went from ~5 pg/mL up to ~185 pg/mL (Figure **3C**), suggesting a strong pro-inflammatory microenvironment in HCECs. Treatment with OP-EVs greatly reduced the LPS-induced inflammatory response. Compared to LPS-stimulated cells, IL-8 secretion dropped to around 445 pg/mL, whereas IL-6 and TNF-α levels were lowered to roughly 195 and 80 pg/mL, respectively (Figure **3A-C**). TNF-α showed the highest reduction after OP-EV treatment, indicating that the anti-inflammatory effect of OP-EVs may influence diverse inflammatory mediators.

As previously reported by the LC-MS/MS study, the complex phytochemical payload contained within OP-EVs may account for some of the observed anti-inflammatory effects. In particular, the presence of several flavonoids and phenolic compounds, such as baicalein, genistein, quercetin glycosides, and ferulic acid, have previously been reported to modulate inflammatory signaling by inhibiting the TLR4/NF-κB and MAPK pathways [36,37]. This reduces the expression of IL-6, IL-8, and TNF-α.

However, the underlying molecular mechanisms responsible for the effects observed in the present study remain to be elucidated. The combined phytochemical composition of OP-EVs and their efficient cellular uptake may contribute to the decrease in LPS-induced cytokine production.

Taken together, these findings show that OP-EVs reduce the inflammatory response caused by LPS in intestinal epithelial cells, which supports their further research as naturally derived nanotherapeutic

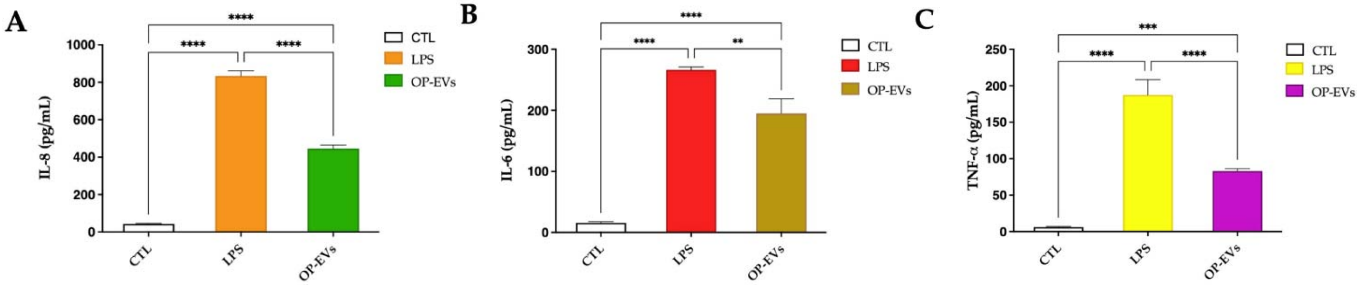

Figure 3: Down-regulation of LPS-induced pro-inflammatory cytokine release by OP-EVs in HCECs. Quantitative ELISA determination of secreted **(A)** Interleukin-8 (IL-8), (**B**) Interleukin-6 (IL-6), and (**C**) Tumor Necrosis Factor-alpha (TNF-α) levels in supernatant collected from HCECs under control conditions (CTL), LPS (1 µg/mL), or LPS co-treated with OP-EV. Data are expressed as mean ± SEM from n = 3 independent biological replicates (**p < 0.01, ***p < 0.001, ****p < 0.0001).

platforms for the treatment of inflammatory bowel disease.

3.4. OP-EVs Promote Epithelial Wound Closure under Inflammatory Conditions

The destruction of epithelial integrity and delayed healing of mucosal ulcers are structural hallmarks of advanced IBD, making intestinal epithelial barrier repair a primary therapeutic goal [2]. To study whether OP-EVs promote epithelial repair, an *in vitro* scratch wound-healing assay was conducted on HCECs under both basal and LPS-induced inflammatory conditions. Wound closure was observed using optical microscopy over a 24-hour period at defined intervals (0, 12, and 24 hours) and quantified as a percentage of closure (Figure **4**).

Untreated HCECs exhibited the expected physiological migratory behavior under normal condition, achieving partial closure of approximately 70.2% at 12 hours and completing the repair (96.1%) within 24 hours. Conversely, after LPS stimulation, the migratory capacity was visibly compromised, resulting in the lowest rate of wound closure across the analyzed timeline (Figure **4B**). This impairment is consistent with the inhibitory effect of inflammatory stimuli on epithelial cell migration and wound repair [38].

The administration of OP-EVs enhanced the healing kinetics under inflammatory settings. At 12 hours, OP-EV-treated cells had 65.9% wound closure, which was comparable to untreated control cells. After 24 hours, OP-EV treatment enhanced wound closure to 84.7%, equal to an almost full closure of the scratched region and a significant improvement compared to the inflammatory control (44.9%).

The improved epithelial healing observed after OP-EVs treatment could be attributed, at least in part, to the complex phytochemical cargo. Flavonoids and phenolic compounds have previously been shown to promote epithelial restitution by inhibiting inflammatory signaling and promoting epithelial migration [39]. Consistently, plant-derived extracellular vesicles have also been reported to promote wound-healing processes, including vesicles derived from *Opuntia Ficus-indica* [34]. Together with the effective cellular uptake shown in Figure **2** and the marked reduction in pro-inflammatory cytokine release shown in Figure **3**, these findings suggest that the bioactive cargo of OP-EVs may contribute to the pro-reparative effects.

OP-EVs may have potential as naturally produced nanotherapeutic platforms for improving intestinal mucosal repair in inflammatory bowel disease, warranting further investigation in more complex models of intestinal inflammation.

3.5. OP-EVs Attenuate Acute NF-κB Signaling in LPS-Stimulated HCECs

The intestinal epithelium is constantly exposed to microbial-derived compounds that contribute to the

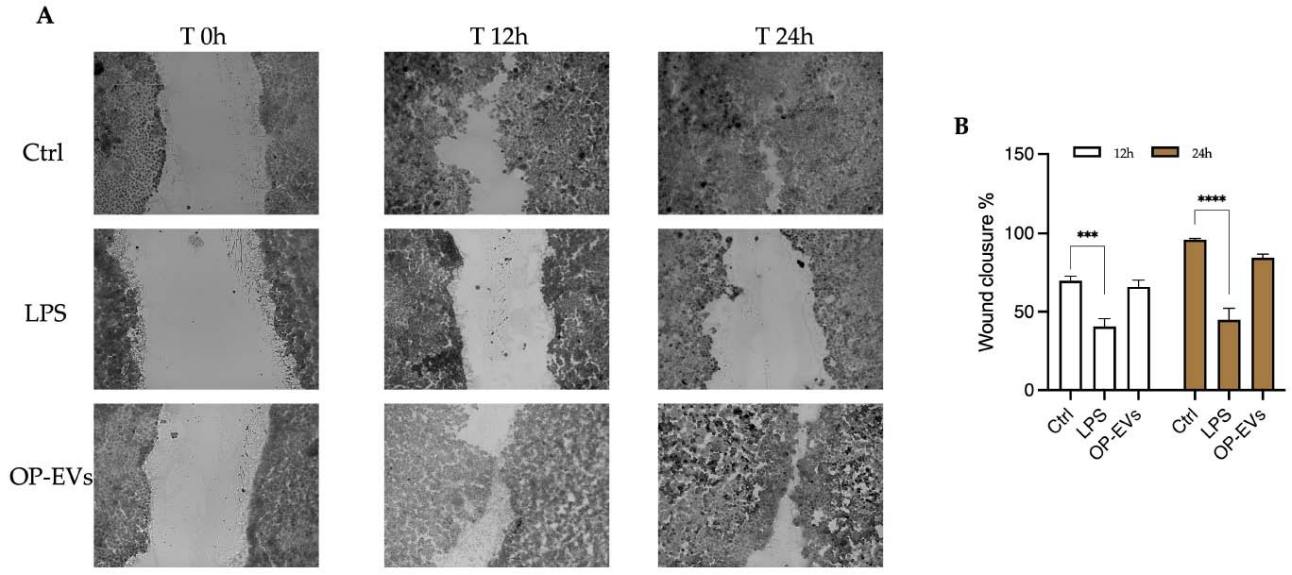

Figure 4: Cell migration kinetics and quantification of OP-EV-induced wound healing. (A) Representative optical microscopy images of scratch wound closure in untreated cells (CTL), LPS-stimulated cells (LPS), and OP-EV-treated cells at 0, 12, and 24 h. (**B**) Quantification of wound closure expressed as percentage of wound closure after 12 and 24 h. Data are presented as mean ± SEM from n = 3 independent biological replicates. (**p < 0.01, ***p < 0.001, **p < 0.0001).

development and progression of intestinal IBD. LPS activates the NF-κB and MAPK/ERK signaling pathway, leading to the production of pro-inflammatory mediators. Persistent stimulation of these pathways causes epithelial dysfunction and barrier damage during the early stages of intestinal inflammation [40-42].

In order to determine if OP-EVs impact the early intracellular inflammatory response, HCECs were stimulated with LPS and NF-κB pathway activation was examined by Western blot analysis of p65 phosphorylation subunit at different time points (Figure **5A**).

LPS stimulated the canonical NF-κB pathway, resulting in a progressive increase in p65 phosphorylation that reached a maximum after about 60 minutes. Total NF-κB levels remained rather steady. Densitometric measurement of the p-NF-κB/NF-κB ratio revealed considerable pathway activation compared to untreated cells (Figure **5B**).

Co-treatment with OP-EVs dramatically reduced NF-κB activation and p65 phosphorylation relative to LPS-stimulated cells. Although phosphorylation was not totally eliminated, the significant reduction shows that OP-EVs effectively attenuate the early inflammatory signaling cascade caused by endotoxin exposure.

Inhibiting p65 phosphorylation may explain why OP-EV-treated HCECs exhibit less inflammation, as NF-κB is a key transcriptional regulator of these cytokines.

Since ERK1/2 signaling is rapidly activated downstream of TLR4 stimulation, we investigated the phosphorylation state of ERK under the identical experimental conditions. LPS significantly increased ERK phosphorylation, which was accompanied by alterations in the p-ERK/ERK ratio, demonstrating MAPK pathway activation during acute inflammatory stimulation [44]. Treatment with OP-EVs markedly reduced ERK activation, restoring phosphorylation levels to those of untreated cells (Figure **5C-5D**). These data show that OP-EVs can affect both NF-κB and MAPK signaling during the early phase of inflammation.

These findings are consistent with previous studies showing that plant-derived extracellular vesicles and flavonoid-rich nanovesicles attenuate NF-κB and MAPK/ERK activation in intestinal inflammatory models [14,44]. Extracellular vesicles generated from plants, in particular, have been suggested as interesting options for IBD due to their capacity to transfer bioactive compounds to target cells and control inflammatory signals [14]. The anti-inflammatory activity of Allium cepa-derived nanovesicles has also been demonstrated by onion-derived nanoparticles inhibiting LPS-induced nitric oxide (NO) production in RAW264

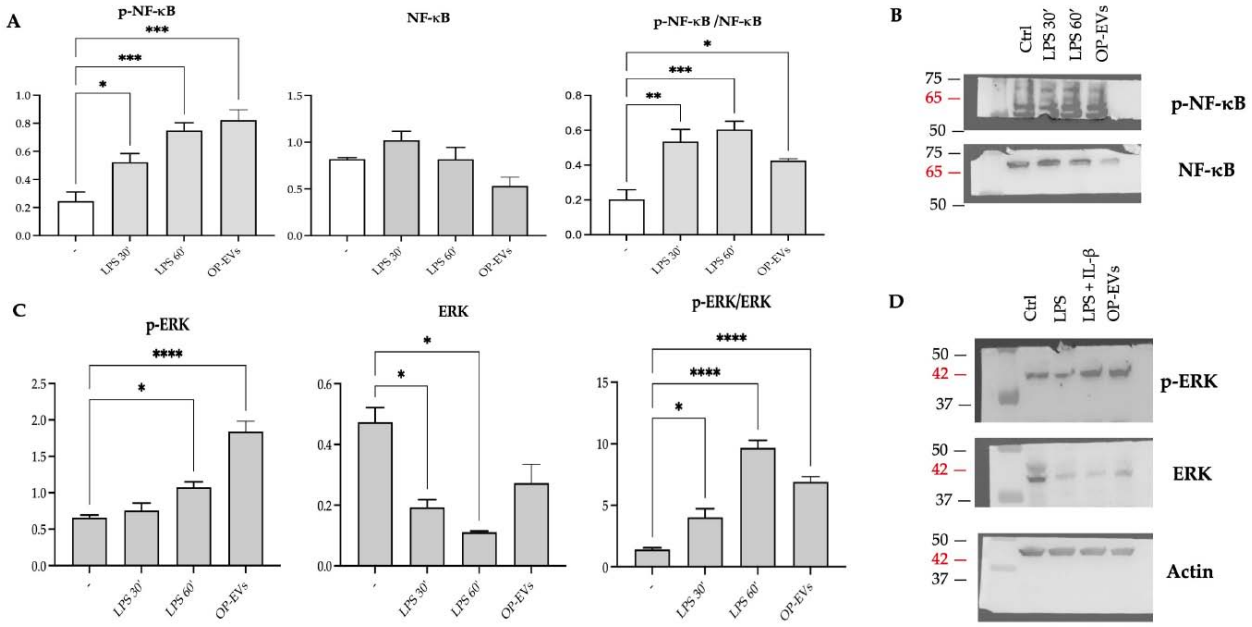

Figure 5: OP-EVs attenuate acute NF-κB and ERK signaling in LPS-stimulated HCECs. (**A-C**) Representative Western blots showing the time-dependent phosphorylation of NF-κB p65 and ERK1/2 in HCECs stimulated with LPS in the absence or presence of OP-EVs. Total NF-κB, total ERK1/2 and β-actin were used as loading controls. (**B–D**) Densitometric quantification of the p-NF-κB/NF-κB and p-ERK/ERK ratios, respectively. Data are presented as mean ± SEM from n = 3 independent biological replicates. (*p < 0.05, **p < 0.01, ***p < 0.001, **** p < 0.0001).

cells [17]. The current work assesses the response of human intestinal epithelial cells, which constitute a crucial biological component of the intestinal barrier, in contrast to earlier onion-derived nanoparticle investigations that were mostly conducted in macrophage models.

The anti-inflammatory activity of OP-EVs may be related to the combined action of their several encapsulated flavonoids, including genistein, baicalein, quercetin derivatives, and ferulic acid. Several of these compounds have independently been associated with modulation of NF-κB and MAPK signaling and inflammatory responses [23-27,36]. Although the contribution of individual metabolites cannot be established in the present study, the observed effects should be interpreted as the potential result of the combined activity of multiple vesicle-associated phytochemicals rather than as evidence for the activity of any single compound.

3.6. OP-EVs Preserve Epithelial Integrity Under Chronic Cytokine-Induced Inflammatory Conditions

Whereas acute inflammatory signaling triggers the intestinal inflammatory response, chronic intestinal inflammation gradually degrades epithelial barrier integrity through changes in cell-cell adhesion and tissue remodeling.

To mimic the chronic inflammatory milieu, HCECs were exposed to a cytokine cocktail of IFN-γ and IL-1β, then treated with OP-EVs. The effects on ERK signaling and epithelial junction proteins were then assessed by Western blot analysis (Figure **6**).

In chronic inflammatory situations, cytokine stimulation changed ERK signaling compared to untreated cells. Interestingly, OP-EV therapy significantly restored ERK activation, as seen by an increase in the p-ERK/ERK ratio (Figure **6A**). Because ERK signaling regulates epithelial migration, proliferation, and tissue repair [45], its recovery suggests that OP-EVs enhance intracellular pathways involved in epithelial restitution rather than inflammatory amplification.

The protective impact of OP-EVs was further highlighted by the modulation of epithelial junction proteins. Exposure to IFN-γ and IL-1β produced a characteristic "cadherin switch", a hallmark of inflammatory epithelial-to-mesenchymal transition

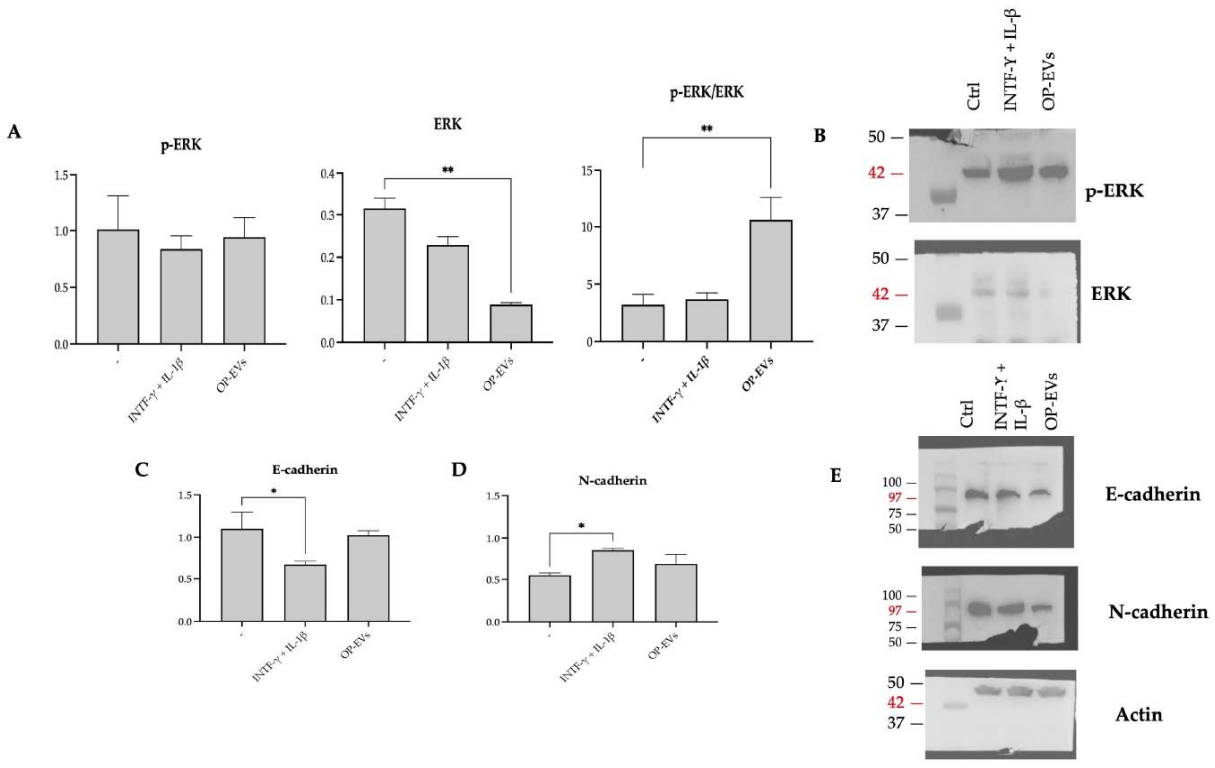

Figure 6. **OP-EVs preserve epithelial integrity under chronic inflammatory conditions.** (**A-B**) Representative Western blots and densitometric analysis of ERK1/2 phosphorylation in HCECs stimulated with IFN-γ/IL-1β in the absence or presence of OP-EVs. (**C-E)** Representative Western blots and densitometric quantification of E-cadherin and N-cadherin expression. Protein levels were normalized to β-actin and expressed relative to untreated controls. Data are presented as mean ± SEM from n = 3 independent biological replicates (*p < 0.05, **p < 0.01).

(EMT) and barrier disintegration, decreasing E-cadherin expression while increasing N-cadherin levels (Figure **6C-6D**).

OP-EV treatment restored E-cadherin expression while decreasing N-cadherin levels to those reported in untreated cells. These findings suggest that OP-EVs may help preserve epithelial cell-cell adhesion and counteract inflammation-induced junctional remodeling. The restoration of E-cadherin and reduction of N-cadherin are consistent with previous reports describing the ability of plant-derived extracellular vesicles to protect intestinal barrier function during inflammatory injury [46,47].

Overall, the combined modulation of ERK signaling and epithelial junction proteins provides a molecular explanation for the improved wound closure observed in the scratch assay, consistent with the established role of ERK signaling in epithelial migration and tissue repair [45] and with evidence supporting the wound-healing potential of flavonoids [39]. These findings suggest that the effects of OP-EVs may extend beyond the suppression of inflammatory mediators to the preservation of epithelial homeostasis and repair, supporting their potential as a promising therapeutic strategy for further investigation in chronic inflammatory conditions.

The bioactivity observed for OP-EVs aligns with early research on edible plant-derived extracellular vesicles in intestinal inflammation. Grape-derived nanovesicles have been shown to target intestinal stem cells and accelerate mucosal tissue renewal in colitis models [48], whereas ginger-derived nanoparticles significantly reduce intestinal inflammation and colitis-associated pathogenesis by inhibiting pro-inflammatory cascades [49]. These well-established studies support the idea that plant vesicles are effective natural delivery mechanisms capable of modulating signaling pathways in the intestinal mucosa.

3.7. OP-EVs Preserve Epithelial Integrity Under Chronic Cytokine-Induced Inflammatory Conditions

From a translational perspective, the use of onion processing waste as a source of OP-EVs provides a promising starting material for scalable and sustainable production. However, several challenges must be overcome before they may be developed into pharmaceutical or nutraceutical products. The reproducibility of the isolation process, which includes enzymatic digestion, differential centrifugation, ultracentrifugation, and ultrafiltration, should be carefully optimized on a larger scale to ensure consistent particle yield, physicochemical characteristics, and phytochemical composition across production batches. Furthermore, the storage stability of OP-EVs should be carefully evaluated by monitoring particle size, concentration, vesicle-associated markers, and phytochemical cargo throughout long-term storage and following freeze-thaw cycles. The use of standardized starting material and controlled processing conditions will also be important to reduce batch-to-batch variability associated with the natural origin of onion peels. Additional manufacturing considerations include developing more scalable purification approaches. These aspects will require further improvement and validation in future studies before OP-EVs can be considered for pharmacological or nutraceutical purposes.

4. CONCLUSIONS

In conclusion, this work shows that nanovesicles derived from onion (*Allium cepa*) processing waste represent a promising, sustainable, and zero-waste source of bioactive nanovesicles with potential for further investigation in the context of inflammatory bowel disease (IBD). Characterized by a mean hydrodynamic diameter of approximately 94 nm, the presence of plant exosome-like markers, and a rich cargo of bioactive polyphenols, the nanovesicles demonstrated high cytocompatibility and were readily internalized by human colonon epithelial cells. In acute LPS-induced inflammation, OP-EV treatment successfully reduced the release of pro-inflammatory cytokines (IL-8, IL-6, and TNF-α), concomitant with attenuation of NF-κB and MAPK/ERK signaling pathways. Additionally, under chronic inflammatory conditions, OP-EVs improved epithelial repair and promoted the restoration of the epithelial barrier associated features, as indicated by increased E-cadherin and reduced N-cadherin expression. Overall, our findings highlight the biological and environmental potential of OP-EVs as an innovative adjuvant approach to promote intestinal health. Further studies, particularly *in vivo* models of intestinal inflammation, are required to determine whether the biological effects observed *in vitro* translate into therapeutic potential *in vivo* and to clarify the contribution of individual vesicle-associated phytochemicals.

AUTHOR CONTRIBUTIONS

Conceptualization, A.C. and R.C.; methodology, F.S., A.V., R.C..; validation, F.S., R.C. and A.V.; formal

APPENDIX

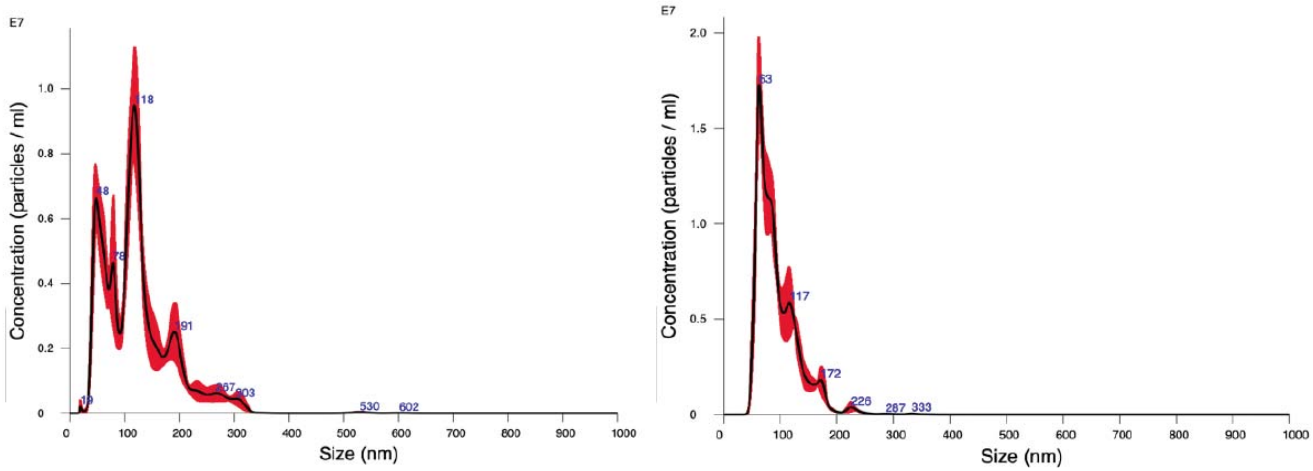

Figure A1. NTA characterization of OP-EVs before and after ultrafiltration. Representative nanoparticle tracking analysis (NTA) profiles showing the particle size distribution and concentration of the OP-EV preparation before ultrafiltration (after enzymatic treatment) and after the ultrafiltration step. The post-ultrafiltration preparation corresponds to the OP-EV sample used for the subsequent physicochemical and biological characterization. The pre-ultrafiltration preparation showed a mean particle diameter of 121.9 nm and a particle concentration of 7.63×10^8 particles/mL, whereas the final post-ultrafiltration preparation showed a mean diameter of 94.1 nm and a concentration of 8.37×10^8 particles/mL. The post-ultrafiltration preparation was used for subsequent physicochemical characterization and biological experiments.

analysis, F.S., A.V., L.M; investigation, F.S., A.V., R.C.; resources, A.C.; data curation,S.M, O.P, Y.L.; writing—original draft preparation, F.S.; writing—review and editing, A.V., R.C., F.S.; visualization, A.C., D.B.; supervision, A.C., D.B.; project administration, O.P; funding acquisition, A.C. All authors have read and agreed to the published version of the manuscript.

FUNDING

This research received no external funding.

INSTITUTIONAL REVIEW BOARD STATEMENT

Not applicable.

INFORMED CONSENT STATEMENT

Not applicable.

DATA AVAILABILITY STATEMENT

The data presented in this study are available on request from the corresponding author.

ACKNOWLEDGEMENTS

The authors gratefully acknowledge Dino Della Torre - Natalí Prodotti Cilentani (Via Roma 8, Vatolla, Perdifumo, Salerno, Italy) for supplying the onion (*Allium cepa* L.) samples required for this research.

CONFLICTS OF INTEREST

The authors declare no conflicts of interest.

REFERENCES

[1] Heydari K, Rahnavard M, Ghahramani S, Hoseini A, Alizadeh-Navaei R, Rafati S, Raei M, Vahidipour M, Salehi F, Motafeghi F, Neshat S, Moosazadeh M, Yousefi M, Pourali A, Rasouli K, Shokrirad S, Lotfi P, Beladi SA, Hadizadeh Neisanghalb M, Sheydaee F, Moghadam S. Global prevalence and incidence of inflammatory bowel disease: a syste--matic review and meta-analysis of population-based studies. Gastroenterol Hepatol Bed Bench 2025; 18(2): 132-146. https://doi.org/10.22037/ghfbb.v18i2.3105

[2] Yang X, Guo H, Zou M. Inflammatory bowel diseases: pathological mechanisms and therapeutic perspectives. Mol Biomed 2026; 7(1): 2. https://doi.org/10.1186/s43556-025-00395-z

[3] Ramos GP, Papadakis KA. Mechanisms of Disease: Inflammatory Bowel Diseases. Mayo Clin Proc 2019; 94(1): 155-165. https://doi.org/10.1016/j.mayocp.2018.09.013

[4] Gieryńska M, Szulc-Dąbrowska L, Struzik J, Mielcarska MB, Gregorczyk-Zboroch KP. Integrity of the Intestinal Barrier: The Involvement of Epithelial Cells and Microbiota-A Mutual Relationship. Animals (Basel) 2022; 12(2): 145. https://doi.org/10.3390/ani12020145

[5] Ghosh S, Whitley CS, Haribabu B, Jala VR. Regulation of Intestinal Barrier Function by Microbial Metabolites. Cellular and Molecular Gastroenterology and Hepatology 2021; 11(5): 1463-1482. https://doi.org/10.1016/j.jcmgh.2021.02.007

[6] Shabani M, Ghoshehy A, Mottaghi AM, Chegini Z, Kerami A, Shariati A, Taati Moghadam M. The relationship between gut microbiome and human diseases: mechanisms, predisposing factors and potential intervention. Front Cell Infect Microbiol 2025; 15: 1516010. https://doi.org/10.3389/fcimb.2025.1516010

[7] Saez A, Herrero-Fernandez B, Gomez-Bris R, Sánchez-Martinez H, Gonzalez-Granado JM. Pathophysiology of Inflammatory Bowel Disease: Innate Immune System. Int J Mol Sci 2023; 24(2): 1526. https://doi.org/10.3390/ijms24021526

[8] Cai Z, Wang S, Li J. Treatment of Inflammatory Bowel Disease: A Comprehensive Review. Front Med (Lausanne) 2021; 8: 765474. https://doi.org/10.3389/fmed.2021.765474

[9] Liu CY, Cham CM, Chang EB. Epithelial wound healing in inflammatory bowel diseases: the next therapeutic frontier. Transl Res 2021; 236: 35-51. https://doi.org/10.1016/j.trsl.2021.06.001

[10] Zhang Y, Liu Y, Liang X, Wen Y, Zhao J, He Y, Xie Q, Xie C. Intestinal barrier in chronic gut and liver diseases: Pathogenesis and therapeutic targets. Acta Pharm Sin B 2025; 15(11): 5515-5536. https://doi.org/10.1016/j.apsb.2025.08.028

[11] Salomon C, Das S, Erdbrügger U, Kalluri R, Kiang Lim S, Olefsky JM, Rice GE, Sahoo S, Andy Tao W, Vader P, Wang Q, Weaver AM. Extracellular Vesicles and Their Emerging Roles as Cellular Messengers in Endocrinology: An Endocrine Society Scientific Statement. Endocr Rev 2022; 43(3): 441-468. https://doi.org/10.1210/endrev/bnac009

[12] Xiang H, Bao C, Chen Q, Gao Q, Wang N, Gao Q, Mao L. Extracellular vesicles (EVs)' journey in recipient cells: from recognition to cargo release. J Zhejiang Univ Sci B 2024; 25(8): 633-655. https://doi.org/10.1631/jzus.B2300566

[13] Di Liu, Jingxian Gao, Xueling Wu, Lu Han, Plant-derived exosome-like nanoparticles as promising biotherapeutic tools: recent advances and challenges. Smart Materials in Medicine 2025; 6(2): 285-304. https://doi.org/10.1016/j.smaim.2025.07.003

[14] Li DF, Tang Q, Yang MF, Xu HM, Zhu MZ, Zhang Y, Tian CM, Nie YQ, Wang JY, Liang YJ, Wang LS, Yao J. Plant-derived exosomal nanoparticles: potential therapeutic for inflammatory bowel disease. Nanoscale Adv 2023; 5(14): 3575-3588. https://doi.org/10.1039/d3na00093a

[15] Bouqbis L, Elomri A, Zair T. Allium cepaL. Peels: Phytochemical Characterization and Bioactive Potential in Infectious and Metabolic Contexts (In vitro, In vivo, and In Silico). Pharmaceutics 2026; 18(4): 476. https://doi.org/10.3390/pharmaceutics18040476

[16] Chen Y, Xu L, Yu Y, Xu Z, Xiao S, Mai H. Protocol for isolating plant-derived extracellular vesicles. STAR Protoc 2026; 7(1): 104379. https://doi.org/10.1016/j.xpro.2026.104379

[17] Yamasaki M, Yamasaki Y, Furusho R, Kimura H, Kamei I, Sonoda H, Ikeda M, Oshima T, Ogawa K, Nishiyama K. Onion (Allium cepa L.)-Derived Nanoparticles Inhibited LPS-Induced Nitrate Production, However, Their Intracellular Incorporation by Endocytosis Was Not Involved in This Effect on RAW264 Cells. Molecules 2021; 26(9): 2763. https://doi.org/10.3390/molecules26092763

[18] Özkan İ, Koçak P, Yıldırım M, Ünsal N, Yılmaz H, Telci D, Şahin F. Garlic (Allium sativum)-derived SEVs inhibit cancer cell proliferation and induce caspase mediated apoptosis. Sci Rep 2021; 11(1): 14773. https://doi.org/10.1038/s41598-021-93876-4

[19] Qi W, Yang L, Pan Y, Lv K, Zhao L, Zhang Y, Kai G, Sun Y, Pan H, Wang D. Chinese leek-derived extracellular vesicles ameliorate sarcopenia by regulating mitochondrial biogenesis and autophagy via AMPK and maintaining myosin homeostasis. J Nanobiotechnology 2025; 23(1): 721. https://doi.org/10.1186/s12951-025-03764-6

[20] Seo N, Ichiki T. Negative Surface Charge and Membrane Lipid Composition Underlying Extracellular Vesicle Function. ACS Nano Med 2026; 1(4): 791-805. https://doi.org/10.1021/acsnanomed.5c00108

[21] Jacob S, Kather FS, Boddu SHS, Rao R, Nair AB. Vesicular Carriers for Phytochemical Delivery: A Comprehensive Review of Techniques and Applications. Pharmaceutics 2025; 17(4): 464. https://doi.org/10.3390/pharmaceutics17040464

[22] Yousefi A, Shadnoush M. Encapsulation Systems for Delivery of Flavonoids: A Review. Biointerface Research in Applied Chemistry 2021; 11(6): 13934-13951. https://doi.org/10.33263/BRIAC116.1393413951

[23] Goh YX, Jalil J, Lam KW, Husain K, Premakumar CM. Genistein: A Review on its Anti-Inflammatory Properties. Front Pharmacol 2022; 13: 820969. https://doi.org/10.3389/fphar.2022.820969

[24] Manikyam HK, Joshi SK. Network Pharmacology of Baicalein Targeting TNF Signaling in Inflammation [J]. Diseases & Research 2025; 5(4): 172-180. https://doi.org/10.54457/DR.202503005

[25] Mueller M, Hobiger S, Jungbauer A, Anti-inflammatory activity of extracts from fruits, herbs and spices, Food Chemistry 2010; 122(4): 987-996. https://doi.org/10.1016/j.foodchem.2010.03.041

[26] Piva M, Martelossi-Cebinelli G, Mendes-Pierotti S, Chinen WH, Cardines PHF, Martinez RM, Georgetti SR, Baracat MM, Vicentini FTMC, Verri WA, *et al*. Flavonoids as Nutraceuticals to Treat Inflammatory Diseases: Focusing on Quercetin, Kaempferol, Luteolin, Apigenin, Epicatechin and Their Effects on Hepatic, Nervous, and Pulmonary Systems. Foods 2026; 15: 2159. https://doi.org/10.3390/foods15122159

[27] Liu J, Guan Y, Yang L, Fang H, Sun H, Sun Y, Yan G, Kong L, Wang X. Ferulic Acid as an Anti-Inflammatory Agent: Insights into Molecular Mechanisms, Pharmacokinetics and Applications. Pharmaceuticals (Basel) 2025; 18(6): 912. https://doi.org/10.3390/ph18060912

[28] Koch BL, Gardner D, Smith H, Bracewell R, Awdey L, Foster J, Borniego ML, Munch DH, Nielsen ME, Pasupuleti R, Trinidad J, Rutter B, Thordal-Christensen H, Innes RW. Molecular insights into the production of extracellular vesicles by plants, Plant Physiology 2026; 200(2): kiag011. https://doi.org/10.1093/plphys/kiag011

[29] Zuppini F, Renzullo L, Tornatore F, Poggio P, Brancaccio M. Heat shock proteins at the crossroads of endosomal trafficking pathways. Cell Biol Toxicol 2025 Dec 11; 41(1): 162. https://doi.org/10.1007/s10565-025-10101-y

[30] Tan XH, Fang D, Xu YD, Nan TG, Song WP, Gu YY, Gu SJ, Yuan YM, Xin ZC, Zhou LQ, Guan RL, Li XS. Skimmed Bovine Milk-Derived Extracellular Vesicles Isolated via "Salting-Out": Characterizations and Potential Functions as Nanocarriers. Front Nutr 2021; 8: 769223. https://doi.org/10.3389/fnut.2021.769223

[31] Chen L, Chen W, Chen H, Guo M, Du W, Wang S, Lao T, Lin H, Shi Y, Pan G, Tian J, Fan Z, Chen F, Liu C. Edible Plant-Derived Extracellular Vesicles: Emerging Nanocarriers for Regenerative Medicine. Journal of Future Foods 2026. https://doi.org/10.1016/j.jfutfo.2026.04.018

[32] Sánchez-López CM, Manzaneque-López MC, Pérez-Bermúdez P, Soler C, Marcilla A. Characterization and bioactivity of extracellular vesicles isolated from pomegranate. Food Funct 2022; 13(24): 12870-12882. https://doi.org/10.1039/d2fo01806c

[33] You JY, Kang SJ, Rhee WJ. Isolation of cabbage exosome-like nanovesicles and investigation of their biological activities in human cells. Bioact Mater 2021; 6(12): 4321-4332. https://doi.org/10.1016/j.bioactmat.2021.04.023

[34] Valentino A, Conte R, Bousta D, Bekkari H, Di Salle A, Calarco A, Peluso G. Extracellular Vesicles Derived from Opuntia ficus-indica Fruit (OFI-EVs) Speed Up the Normal Wound Healing Processes by Modulating Cellular Responses. Int J Mol Sci 2024; 25(13): 7103. https://doi.org/10.3390/ijms25137103

[35] Neurath MF. Cytokines in inflammatory bowel disease. Nat Rev Immunol 2014; 14(5): 329-42. https://doi.org/10.1038/nri366.1

[36] Zhong R, Miao L, Zhang H, Tan L, Zhao Y, Tu Y, Angel Prieto M, Simal-Gandara J, Chen L, He C, Cao H. Anti-inflammatory activity of flavonols viainhibiting MAPK and NF-κB signaling pathways in RAW264.7 macrophages. Curr Res Food Sci 2022; 5: 1176-1184. https://doi.org/10.1016/j.crfs.2022.07.007

[37] Alhelwani S, Degirmenci NS, Altıntaş CM, *et al*. Comparative Analysis of Red Onion-Derived Exosome-Like Nanovesicles and Extract Reveals Sustained Immunomodulatory Effects in LPS/IFN-γ-Stimulated Microglia. Mol Neurobiol 2026; 63: 533. https://doi.org/10.1007/s12035-026-05820-0

[38] Ivanov AI, Parkos CA, Nusrat A. Cytoskeletal regulation of epithelial barrier function during inflammation. Am J Pathol 2010; 177(2): 512-24. https://doi.org/10.2353/ajpath.2010.100168

[39] Zulkefli N, Che Zahari CNM, Sayuti NH, Kamarudin AA, Saad N, Hamezah HS, Bunawan H, Baharum SN, Mediani A, Ahmed QU, Ismail AFH, Sarian MN. Flavonoids as Potential Wound-Healing Molecules: Emphasis on Pathways Perspective. Int J Mol Sci 2023; 24(5): 4607. https://doi.org/10.3390/ijms24054607

[40] Jergens AE, Parvinroo S, Kopper J, Wannemuehler MJ. Rules of Engagement: Epithelial-Microbe Interactions and Inflammatory Bowel Disease. Front Med (Lausanne) 2021; 8: 669913. https://doi.org/10.3389/fmed.2021.669913

[41] Page MJ, Kell DB, Pretorius E. The Role of Lipopolysaccharide-Induced Cell Signalling in Chronic Inflammation. Chronic Stress (Thousand Oaks) 2022; 6: 24705470221076390. https://doi.org/10.1177/24705470221076390

[42] Gao J, Cao B, Zhao R, Li H, Xu Q, Wei B. Critical Signaling Transduction Pathways and Intestinal Barrier: Implications for Pathophysiology and Therapeutics. Pharmaceuticals (Basel) 2023; 16(9): 1216. https://doi.org/10.3390/ph16091216

[43] Curson JEB, Liu L, Luo L, Muusse TW, Lucas RM, Gunther KS, Vajjhala PR, Abrol R, Jones A, Kapetanovic R, Stacey KJ, Stow JL, Sweet MJ. TLR4 phosphorylation at tyrosine 672 activates the ERK/c-FOS signaling module for LPS-induced cytokine responses in macrophages. Eur J Immunol 2023; 53(7): e2250056. https://doi.org/10.1002/eji.202250056

[44] Tan F, Liu W, Li T, *et al*. Plant-derived extracellular vesicles as tools and targets for inflammatory diseases. J Nanobiotechnol 2026; 24: 397. https://doi.org/10.1186/s12951-026-04294-5

[45] Samson SC, Khan AM, Mendoza MC. ERK signaling for cell migration and invasion. Front Mol Biosci 2022; 9: 998475. https://doi.org/10.3389/fmolb.2022.998475

[46] Huang D, Chen J, Zhao M, Shen H, Jin Q, Xiao D, Peng Z, Chen T, Zhang Y, Rao D, Liu M. Plant-derived extracellular vesicles: composition, function and clinical potential. J Transl Med 2025; 23(1): 1065. https://doi.org/10.1186/s12967-025-07101-1

[47] Lialios P, Alimperti S. Role of E-cadherin in epithelial barrier dysfunction: implications for bacterial infection, inflammation, and disease pathogenesis. Front Cell Infect Microbiol 2025; 15: 1506636. https://doi.org/10.3389/fcimb.2025.1506636

[48] Ju S, Mu J, Dokland T, Zhuang X, Wang Q, Jiang H, Xiang X, Deng ZB, Wang B, Zhang L, Roth M, Zhang HG. Grape exosome-like vesicles induce intestinal stem cells and protect mice from DSS-induced colitis. Molecular Therapy 2013; 21(7): 1345-1357. https://doi.org/10.1038/mt.2013.64

[49] Zhang M, Viennois E, Prasad M, Zhang Y, Wang L, Zhang Z, Si TY, Xiao B, Merlin D. Edible Ginger-Derived Nanoparticles Protect Against Intestinal Inflammation and Colitis-Associated Cancer. Cell Host & Microbe 2016; 20(2): 212-227. https://doi.org/10.1016/j.chom.2016.07.005